Range Extension Autonomous Driving for Electric Vehicles Based on Optimal Velocity Trajectory Considering Road Gradient Information

Hideki Yoshida[*a)] Student Member, Hiroshi Fujimoto[*] Senior Member

Electric Vehicles (EVs) have been considered as one of the solutions for environmental and energy problems. The mileage per charge of EVs, however, is shorter than that of Internal Combustion Engine Vehicles (ICEVs). In this paper, Range Extension Autonomous Driving (READ) system is proposed by taking the road gradient information into account, and the proposed READ system optimizes velocity trajectory to minimize the energy consumption in the case of autonomous driving. The main contribution of this study is the modeling energy consumption by considering road gradient information and motor loss. Moreover, both simulations and experiments are performed to demonstrate the effectiveness of the proposed method in terms of mileage per charge.

Keywords: electric vehicle, range extension autonomous driving, optimal control, road gradient information

1. Introduction

With the increasing concerns on environmental and energy problems, Electric Vehicles (EVs) have been intensively studied during the past years. EVs have many remarkable advantages over Internal Combustion Engine Vehicles (ICEVs), and three main advantages are listed as below.

(1) The response of torque by motor is much faster than that of engines (100 times) .
(2) In-wheel motors enable independent driving force control.
(3) Motor torque can be measured precisely with motor current.

These advantages are demonstrated to be useful for motion control of EVs [1][2].

However, the short mileage per charge of EVs prevents them from wide spreading to a certain extent. In order to solve this problem, lots of methods were proposed [3]~[7]. For example, a control system was proposed to reduce iron loss by regulating the flux density of motors [3]. Some other research works considered optimization of driving force distribution in terms of motor efficiency [4]~[6]. However, these studies did not consider minimization of the total energy consumption. Meanwhile, there is research on minimizing the amount of total energy consumption considering gradient resistance and velocity constraint. Yet the research does not take account of motor efficiency [7].

The authors' research group has proposed Range Extension Control Systems (RECS) [8][9] and Range Extension Autonomous Driving (READ) using purely motion control techniques [10], which does not change motor type and vehicle structures. The conventional methods are mainly focused on optimizing the velocity trajectory and the distribution of driving forces [10]. READ can improve energy efficiency in autonomous driving systems for highway applications which have been intensively discussed recently [11]. However, important factor such as road gradient resistance are not considered. READ considering road gradient information can be expected to reduce more energy consumption. In this study, road gradient information is assumed to be available from onboard devices such as Global Positioning System (GPS), and the velocity trajectory can be designed by formulating a optimization algorithm. The effectiveness of proposed method is verified by simulations and experiments.

(a) FPEV2-Kanon.

(b) Front motor. (c) Rear motor.

Fig. 1. Experimental vehicle.

2. Experimental Vehicle and Model

2.1 Experimental Vehicle In this research, an original electric vehicle "FPEV2–Kanon" which the authors' research group manufactured is used. The photo and the specification of the vehicle are shown in Fig. 1 and Tab. 1. This

a) Correspondence to: yoshida14@hflab.k.u-tokyo.ac.jp
* The University of Tokyo
5-1-5, Kashiwanoha, Kashiwa, Chiba, 227-8561 Japan

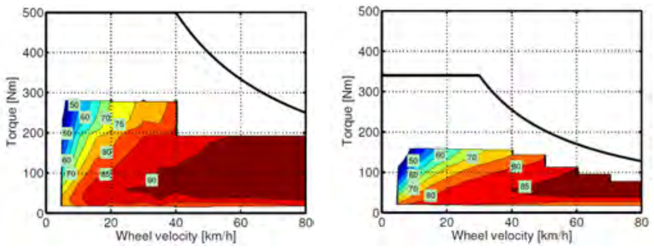

(a) Front motor. (b) Rear motor.

Fig. 2. Efficiency maps of front and rear motors.

Table 1. Vehicle specification.

Vehicle mass M	854 kg
Wheel base l	1.72 m
Distance from CG to front and rear axle l_f, l_r	l_f : 1.01 m l_r : 0.702 m
Front wheel inertia J_{ω_f}	1.24 kgm^2
Rear wheel inertia $J_{\omega r}$	1.26 kgm^2
Wheel radius r	0.302 m

Table 2. Specifications of in-wheel motors.

	Front	Rear
Manufacturer	TOYO DENKI SEIZO K.K.	
Type	Direct drive system Outer rotor type	
Rated torque	110 Nm	137 Nm
Maximum torque	500 Nm	340 Nm
Rated power	6.00 kW	4.30 kW
Maximum power	20.0 kW	10.7 kW
Rated speed	382 rpm	300 rpm
Maximum speed	1110 rpm	1500 rpm

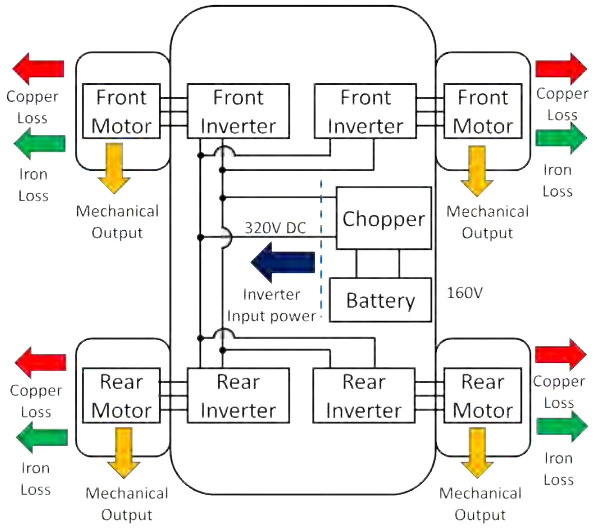

Fig. 3. Power flow diagram.

vehicle has four outer-rotor type in-wheel motors. These motors are direct drive type. Therefore the reaction forces from road are directly transferred to the motor without backlash influence of the reduction gear. Tab. 1 shows the specification of vehicle. Tab. 2 shows the specification of the motors. Fig 2 shows efficiency maps of the front and the rear in-wheel motors. Fig. 3 illustrates energy flow diagram of power system on the vehicle. Lithium-ion battery is used as power source. The voltage of the main battery is 160 V. The

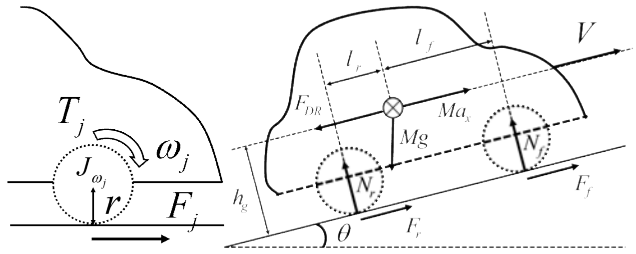

(a) Rotational motion of a wheel. (b) Load transfer model.

Fig. 4. Vehicle model.

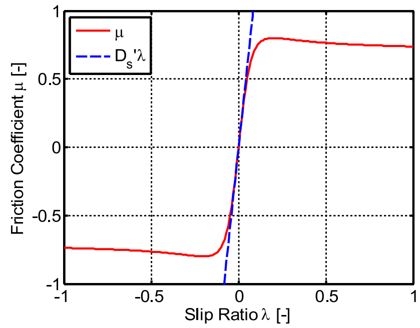

Fig. 5. μ–λ curve [12].

voltage is boosted to 320 V by a chopper. In this paper, the chopper loss is neglected.

2.2 Vehicle Model In this section, a four wheel driven vehicle model is described. Using the model given in Fig. 4(a), the wheel dynamics is expressed as Eq.(1). From Fig. 4(b), the vehicle dynamics are expressed as Eq.(2) and (3)

$$J_{\omega_j}\dot{\omega}_j = T_j - rF_j, \quad \cdots\cdots (1)$$

$$M\dot{V} = F_{\mathrm{all}} - \mathrm{sgn}(V)F_{\mathrm{DR}}(V,\theta) - Mg\sin\theta, \quad \cdots\cdots (2)$$

$$F_{\mathrm{DR}}(V,\theta) = \mu_0 Mg\cos\theta + b|V| + \frac{1}{2}\rho C_{\mathrm{d}} AV^2, \quad \cdots\cdots (3)$$

where ω_j is the wheel angular velocity, V is the vehicle velocity, T_j is the motor torque, F_j is the driving force of each wheel, F_{all} is the total driving force, M is the vehicle mass, r is the wheel radius, J_{ω_j} is the wheel inertia, F_{DR} is the driving resistance, μ_0 is rolling friction coefficient, θ is road gradient, b is resistance vehicle velocity coefficient, ρ is air density, C_{d} is constant drag and A is frontal projected area. The subscript j represents f or r, f stands for “front” and r represents “rear”.

The slip ratio λ_j is defined as

$$\lambda_j = \frac{V_{\omega_j} - V}{\max(V_{\omega_j}, V, \epsilon)}, \quad \cdots\cdots (4)$$

where $V_{\omega_j} = r\omega_j$ is the wheel speed and ϵ is a small constant to avoid zero division. The slip ratio λ_j is known to be related with the coefficient of friction μ_j [12], as shown in Fig. 5. In region $|\lambda_j| \ll 1$, μ_j is nearly proportional to λ_j. Then, for longitudinal acceleration cases,

$$F_j = \mu_j N_j \approx D_s{}' N_j \lambda_j, \quad \cdots\cdots (5)$$

where $D_s{}'$ is the normalized driving stiffness.

In this paper, F_f and F_r are distributed F_{all} equally.

$$F_j = \frac{1}{4}F_{\text{all}}. \quad (6)$$

The normal forces of each wheel during the longitudinal acceleration process are calculated as follows

$$N_f(\dot{V},\theta) = \frac{1}{2}\left[\frac{l_r}{l}Mg\cos\theta - \frac{h_g}{l}M\dot{V}\right], \quad (7)$$

$$N_r(\dot{V},\theta) = \frac{1}{2}\left[\frac{l_f}{l}Mg\cos\theta + \frac{h_g}{l}M\dot{V}\right], \quad (8)$$

where N_f and N_r are respectively the front and rear normal forces, l_f and l_r are respectively the distances from the center of gravity to the front and rear axles, l is the wheelbase, and h_g is the height of the center of gravity. The acceleration direction is defined as positive when the vehicle is accelerating.

2.3 Power Flow Model [10] The inverter input power P_{in} in Fig. 3 considering the slip ratio and motor loss is expressed as

$$P_{\text{in}} = P_{\text{out}} + P_{\text{c}} + P_{\text{i}}, \quad (9)$$

where P_{out} is the sum of the mechanical output of each motor, P_{c} is the sum of the copper loss of each motor, and P_{i} is the sum of the iron loss of each motor, and neglecting the inverter loss and mechanical loss.

When each wheel angular acceleration is small, torque T_j is proportional to driving force. T_j is expressed as

$$T_j \approx rF_j. \quad (10)$$

When the slip ratioλ_j is small enough, ω_j is expressed as

$$\omega_j = \frac{V}{r(1-\lambda_j)} \approx \frac{V}{r}(1+\lambda_j). \quad (11)$$

By substituting Eq.(5) for Eq.(6) and Eq.(11), λ_j is expressed as

$$\lambda_j = \frac{F_j}{D_s{}' N_j(\dot{V},\theta)} = \frac{F_{\text{all}}}{4D_s{}' N_j(\dot{V},\theta)}. \quad (12)$$

Approximate P_{out}, P_{c} and P_{i} are expressed as

$$P_{\text{out}} = 2\sum_{j=f,r}\omega_j T_j = V\frac{F_{\text{all}}}{2}\sum_{j=f,r}\left(1+\frac{F_{\text{all}}}{4D_s{}' N_j(\dot{V},\theta)}\right), \quad (13)$$

$$P_{\text{c}} = \frac{r^2}{2}F_{\text{all}}{}^2\sum_{j=f,r}\frac{R_j}{4K_{tj}{}^2}, \quad (14)$$

$$P_{\text{i}} = 2\frac{V^2}{r^2}\sum_{j=f,r}\frac{P_{nj}{}^2}{R_{cj}}\left[\left(\frac{rL_{qj}F_{\text{all}}}{4K_{tj}}\right)^2 + \Psi_j{}^2\right], \quad (15)$$

where R_j is the armature winding resistance of the motor, K_{tj} is the torque coefficient of the motor, P_{nj} is the number of pole pairs, L_{qj} is the q-axis inductance and Ψ_j is the interlinkage magnetic flux.

The electrical angular velocity of the motor ω_{ej} and the equivalent iron loss resistance R_{cj} are expressed as

$$\omega_{ej} = \frac{P_{nj}V}{r}, \quad (16)$$

$$\frac{1}{R_{cj}} = \frac{1}{R_{c0j}} + \frac{1}{R_{c1j}{}' \left|\omega_{ej}\right|}, \quad (17)$$

where the first and second terms on the right-hand side represent the eddy current loss and hysteresis loss respectively.

Road gradient can be estimated from the distance traveled on condition that grade map data is stored in advance. Therefore, the road gradient function θ can be described by distance traveled X. Then the inverter input power is expressed by V, X and F_{all} as

$$\theta = \theta(X), \quad (18)$$

$$P_{\text{in}}(V, X, F_{\text{all}}) = P_{\text{out}}(V,X,F_{\text{all}}) + P_{\text{c}}(F_{\text{all}}) + P_{\text{i}}(V,F_{\text{all}}). \quad (19)$$

3. Optimization of Velocity Trajectory Considering Road Gradient Information

3.1 The Evaluation Function and the Constraint Condition In this section, on the assumption that the EVs are autonomous driving, we propose READ which calculates optimal velocity trajectory which minimizes the total amount of energy consumption from initial time t_0 to final time t_f. EVs can regenerate kinematic energy and potential energy. Therefore, minimization of total energy consumption is equal to maximization of regenerative energy. The evaluation function and the constraint conditions are described as

$$\text{min.}\ \ W_{\text{in}} = \int_{t_0}^{t_f} P_{\text{in}}(\boldsymbol{x}(t),\boldsymbol{u}(t))dt, \quad (20)$$

$$s.t.\ \ \dot{\boldsymbol{x}}(t) = \boldsymbol{f}(\boldsymbol{x}(t),\boldsymbol{u}(t)), \quad (21)$$

$$\chi(\boldsymbol{x}(t_0)) = \boldsymbol{x}(t_0) - \boldsymbol{x}_0 = \boldsymbol{0}, \quad (22)$$

$$\psi(\boldsymbol{x}(t_f)) = \boldsymbol{x}(t_f) - \boldsymbol{x}_f = \boldsymbol{0}, \quad (23)$$

where

$$\boldsymbol{x}(t) = \begin{bmatrix} V(t) \\ X(t) \end{bmatrix}, \boldsymbol{u}(t) = F_{\text{all}}(t), \quad (24)$$

$$\boldsymbol{f}(\boldsymbol{x}(t),\boldsymbol{u}(t)) = \boldsymbol{f}(V(t),X(t),F_{\text{all}}(t)) = \begin{bmatrix} \frac{1}{M}\{F_{\text{all}}(t) - \text{sgn}(V(t))F_{\text{DR}}(V(t),\theta(X)) - Mg\sin\theta(X)\} \\ V(t) \end{bmatrix}, \quad (25)$$

where $X(t)$ is the distance traveled and $\boldsymbol{x_0}$ is the initial condition of velocity and distance traveled. $\boldsymbol{x_f}$ is the final condition of velocity and distance traveled. Penalty function $P(\boldsymbol{x}(t_f))$ which turns the constrained problem into the unconstrained problem on final condition is described as

$$P(\boldsymbol{x}(t_f)) = \frac{1}{2}\sigma\|\psi(\boldsymbol{x}(t_f))\|^2, \quad (26)$$

where σ is the penalty parameter. Concomitant variable $\boldsymbol{\nu}(t)$ is used to turn the constrained problem into an unconstrained problem using final condition. Then the Hamiltonian function H is described as

$$H(\boldsymbol{x},\boldsymbol{u},\boldsymbol{\nu}) = P_{\text{in}}(\boldsymbol{x},\boldsymbol{u}) + \boldsymbol{\nu}^T\boldsymbol{f}(\boldsymbol{x},\boldsymbol{u}). \quad (27)$$

Therefore, the evaluation function J without constraints is defined as

Table 3. Iron loss specification

R_{c0j}	300 Ω
R'_{c1f}	0.130 Ωs/rad
R'_{c1r}	0.0525 Ωs/rad

$$J = P(\boldsymbol{x}(t_f)) + \int_{t_0}^{t_f} \{H(\boldsymbol{x}, \boldsymbol{u}, \boldsymbol{\nu}) - \boldsymbol{\nu}(t)^T \dot{\boldsymbol{x}}\} dt. \cdots\cdots (28)$$

Euler–Lagrange equations are described as

$$\dot{\boldsymbol{\nu}} = -\left(\frac{\partial H(\boldsymbol{x}, \boldsymbol{u}, \boldsymbol{\nu})}{\partial \boldsymbol{x}}\right)^T, \cdots\cdots (29)$$

$$\boldsymbol{\nu}(t_f) = \left.\frac{\partial P(\boldsymbol{x})}{\partial \boldsymbol{x}}^T\right|_{t=t_f}, \cdots\cdots (30)$$

$$\frac{\partial H(\boldsymbol{x}, \boldsymbol{u}, \boldsymbol{\nu})}{\partial \boldsymbol{u}} = 0. \cdots\cdots (31)$$

Optimal velocity trajectory to minimize the total amount of energy consumption is derived using the steepest descent method that satisfies with Euler–Lagrange equations.

3.2 Comparison Conditions In this section, the velocity trajectories are explained to compare with proposed velocity trajectory.

- **Trajectory 1 Constant Deceleration**
  Trajectory 1 is a conventional method assuming that a driver stops after constant deceleration. The velocity trajectory $V(t)$ and final time t_f are described as

$$V(t) = V_0 - \frac{{V_0}^2}{2X_f} t, \cdots\cdots (32)$$

$$t_f = \frac{2X_f}{V_0}, \cdots\cdots (33)$$

  where V_0 is initial velocity and X_f is final distance traveled.
- **Trajectory 2 Optimized Velocity Trajectory Not Considering Road Gradient Information**
  Trajectory 2 is a conventional method which minimizes energy consumption by autonomous driving, but without considering road gradient. Then road gradient is assumed as $\theta(X) = 0$.
- **Trajectory 3 Optimized Velocity Trajectory Considering Road Gradient Information**
  Trajectory 3 is a proposed method which minimizes energy consumption by autonomous driving, considering road gradient.

4. Simulation

In this section, a simulation on the three trajectories are conducted.

4.1 Simulation Conditions Fig. 6(a) shows the test road at National Traffic Safety and Environment Laboratory. Fig. 6(b) illustrates the road gradient profile of the test road. The simulation conditions are given in Tab. 1–4. The initial condition is given as t_0=0.00 s, V_0=30.0 km/h, X_0=0.00 m. The final condition is given as t_f= 24.7 s, V_f=0.00 km/h, X_f=103 m.

4.2 Control System Vehicle velocity control system is designed to control the EVs velocity automatically. Fig. 7 shows the system which is composed of a feedforward controller and feedback controller. Front and rear torque reference ${T_j}^*$ is given as

Table 4. Driving resistance condition

Rolling friction coefficients μ_0	1.28×10^{-2}
Constant drag C_d	0.806
Frontal projected area A	1.20 m^2
Driving Stiffness $D_s{}'$ (dry asphalt)	12.0

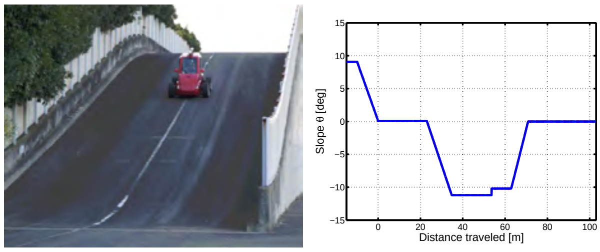

(a) Test road. (b) Road gradient profile.

Fig. 6. Test road and road gradient profile.

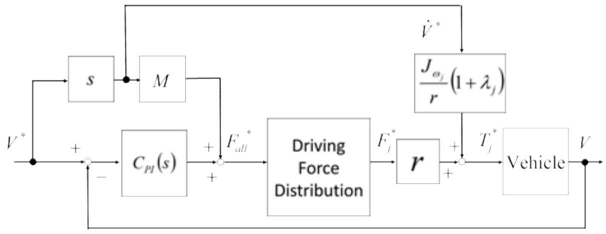

Fig. 7. Velocity control system.

$$T_j{}^* = rF_j{}^* + \frac{J_{\omega_j}\dot{V}^*}{r}(1 + \lambda_j). \cdots\cdots (34)$$

The second term of right hand side compensates inertia of the wheels. Vehicle velocity controller $C_{PI}(s)$ is a PI controller, and it is designed by the pole placement method. The plant of vehicle velocity is expressed as

$$\frac{V}{F_{\rm all}} = \frac{1}{Ms}. \cdots\cdots (35)$$

In the simulation and experiment, the poles of vehicle velocity controller are set to -5 rad/s.

4.3 Simulation Results Simulation results are shown in Fig. 8. Fig. 8(d)–8(f) show the dominant loss of power flow model. The dominant losses are expressed as

$$P_{\rm M} = \frac{d}{dt}\left(\frac{1}{2}MV^2\right) = MV\dot{V}, \cdots\cdots (36)$$

$$P_{\rm DR} = F_{\rm DR}V, \cdots\cdots (37)$$

where $P_{\rm M}$ is the power stored as kinectic energy of the vehicle mass, $P_{\rm DR}$ is the loss caused by the driving resistance.

When vehicle reduces in the speed at a constant deceleration on the downward slope as conventional trajectory 1, motors convert potential energy and kinematic energy to electric energy. Then motors must generate larger total braking force than road gradient resistance. Therefore copper loss becomes large and regenerative energy becomes small.

Conventional trajectory 2 is calculated not considering road gradient information. When the vehicle runs on the flat area from 0.00 to 23.0 m, vehicle reduces speed more quickly than that of conventional trajectory 1 to prevent the vehicle from losing kinematic energy from driving resistance. Then regenerative energy of conventional trajectory 2 is larger than that of conventional trajectory 1. When vehicle runs on the

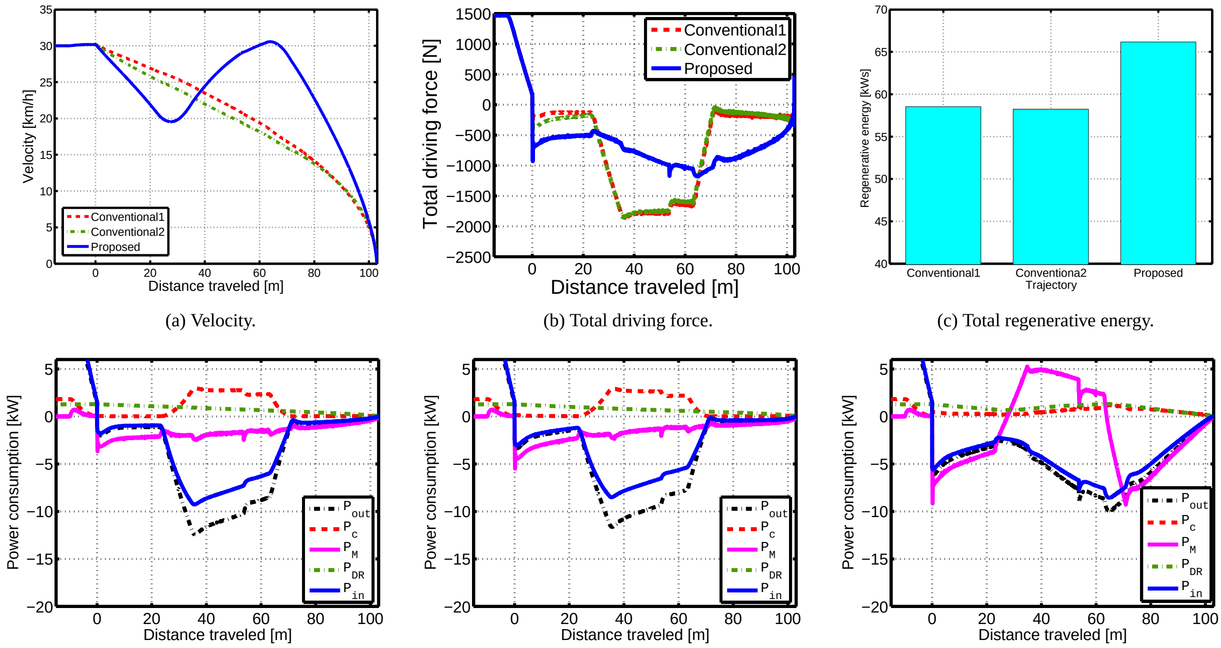

(a) Velocity. (b) Total driving force. (c) Total regenerative energy.

(d) Power consumption (Trajectory 1). (e) Power consumption (Trajectory 2). (f) Power consumption (Trajectory 3).

Fig. 8. Simulation results of pattern driving.

downward slope from 23.0 to 60.0 m, deceleration of conventional trajectory 2 is larger than that of conventional trajectory 1. Then copper loss of conventional trajectory 2 is slightly bit larger than that of conventional trajectory 1.

Proposed trajectory 3 is calculated considering gradient information. On the flat area, the vehicle reduces in speed at an optimal deceleration to prevent the vehicle from losing kinematic energy by driving resistance. On the other hand, copper loss is larger than that of conventional trajectories. On the downward slope, vehicle speeds up at an optimal acceleration to prevent the vehicle from losing potential energy by the copper loss. Then kinematic energy becomes large to regenerate potential energy. Inverter input power of trajectory 3 is larger than that of conventional both conventional trajectory 1 and 2 to suppress copper loss on the flat area.

Fig. 8(c) shows regenerative energy on conventional trajectory 1, 2 and proposed trajectory 3. Regenerative energy of trajectory 1, 2, and 3 are 58.5 kWs, 58.2 kWs, and 66.2 kWs, respectively. Regenerative energy of proposed trajectory improved about 13.0 % compared with that of conventional trajectory 1 and 2. Therefore, the algorithm to maximize regenerative energy should be designed in consideration of two cases: 1) Reduce regenerative braking if it increases the copper loss: 2) Increase regenerative braking in the case it has little influence on the copper loss, i.e., hard braking can reduce driving resistance loss.

5. Experiment

Experiments were conducted on the test road shown in Fig. 6(a) under the same condition as simulation. Vehicle velocity V, inverter input power P_{in}, mechanical output P_{out}, total loss P_{L} including motor copper loss , motor iron loss and inverter loss and driving resistance loss P_{DR} are calculated as

$$V = \frac{r}{4}\sum_{j=f,r}\sum_{i=l,r}\omega_{ij}, \quad (38)$$

$$P_{\mathrm{in}} = V_{\mathrm{dc}}\sum_{j=f,r} I_{\mathrm{dc}j}, \quad (39)$$

$$P_{\mathrm{out}} = \sum_{i=l,r}\sum_{j=f,r}\omega_{ij}T_{ij}, \quad (40)$$

$$P_{\mathrm{L}} = |P_{\mathrm{out}} - P_{\mathrm{in}}|, \quad (41)$$

$$P_{\mathrm{DR}} = F_{\mathrm{DR}}V = \left(F_{\mathrm{all}} - M\dot{V} - Mg\sin\theta\right)V, \quad (42)$$

where the subscript i represents l or r (l stands for left and r represents right wheel). V_{dc} is measured the inverter input voltage and $I_{\mathrm{dc}j}$ is the measured inverter input current. P_{in} includes inverter loss. We assumed that road gradient θ is equal to the measured vehicle pitch angle.

Fig. 9 shows experimental results which are the average values and standard deviations of 5 times experiments. Regenerative energy of trajectory 1, 2, and 3 are 52.6 kWs, 52.6 kWs, and 60.2 kWs, respectively. Regenerative energy of proposed trajectory 3 improved significantly about 14.5 % compared with that of conventional trajectory 1 and 2. The experimental results is consistent with simulation results. Compared to simulation results, Errors of driving force and copper loss are large when distance traveled is around 25.0 m and 70.0 m. Error of distance traveled occurs because the vehicle velocity controller does not control the vehicle position.

6. Conclusions and Future Works

This paper proposed a READ system that can optimally generate vehicle velocity to reduce energy consumption considering road gradient information. In the experiments, it is demonstrated that the proposed method increases regenerative energy by 14 % in comparison with the conventional

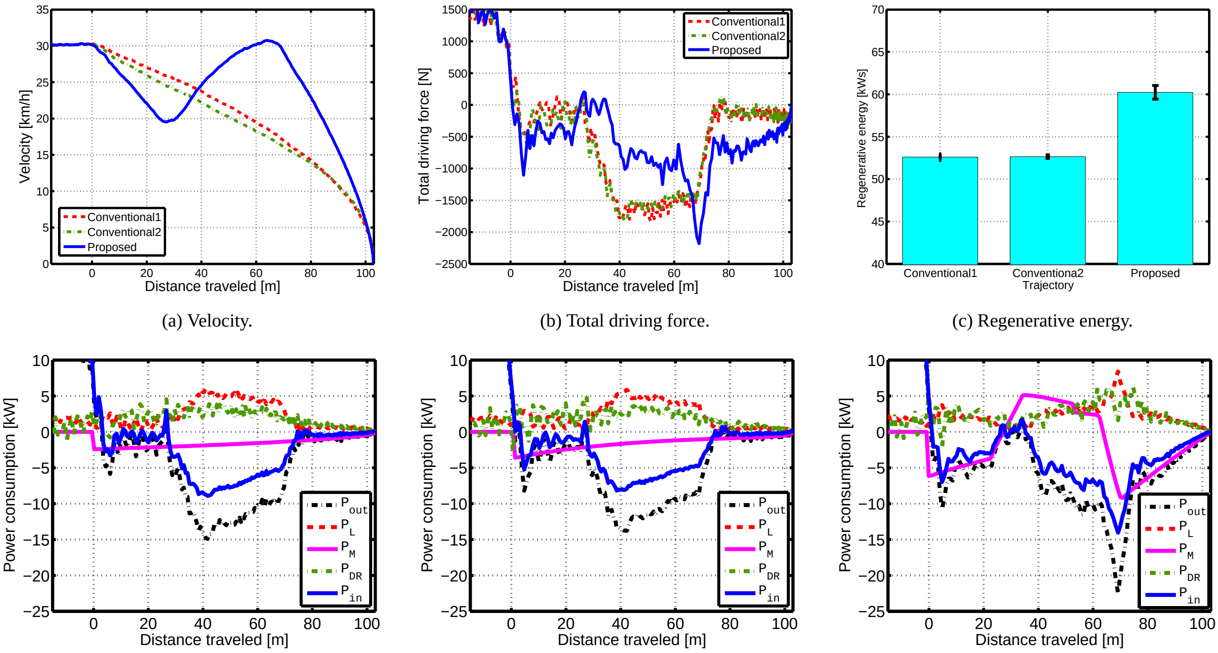

(a) Velocity. (b) Total driving force. (c) Regenerative energy.

(d) Power consumption (Trajectory 1). (e) Power consumption (Trajectory 2). (f) Power consumption (Trajectory 3).

Fig. 9. Experimental results of pattern driving.

READ systems. However, it should be noted that the copper loss was accumulated due to the incorrect information of traveling distance, and to reduce copper loss, it is desirable to include algorithms such as Kalman filter for vehicle velocity or traveling distance estimation.

The future works include: 1) Introduce optimal driving-braking force distribution ratio to the proposed system, 2) Consider constraints on speed and acceleration on general roads and highways.

Acknowledgment

This research was partly supported by Industrial Technology Research Grant Program from New Energy and Industrial Technology Development Organization (NEDO) of Japan (number 05A48701d), and by the Ministry of Education, Culture, Sports, Science and Technology grant (number 22246057 and 26249061). I appreciate the support and advice given by Ono Sokki Co., Ltd. and National Traffic Safety and Environment Laboratory (NTSEL).

References

(1) Y. Hori: "Future Vehicle Driven by Electricity and Control-Research on Four-Wheel-Motored" UOT Electric March II"," IEEE Trans. on Industrial Electronics, Vol. 51, No. 5, pp.954–962 (2004).

(2) K. Maeda, H. Fujimoto and Y. Hori: "Four-wheel Driving-force Distribution Method for Instantaneous or Split Slippery Roads for Electric Vehicle," Automatika - Journal for Control, Measurement, Electronics, Computing and Communications, pp. 103–113 (2013).

(3) H. Hijikata, K. Akatsu, Y. Miyama, H Arita and A. Daikoku: "Suppression Control Method for Iron Loss of MATRIX Motor under Flux Weakening Utilizing Individual Winding Current Control," IPEC-Hiroshima 2014, pp. 2673–2678 (2014).

(4) Y. P. Yang, Y. C. Shih and J. M. Chen: "Real-Time Distribution Strategy for an Electric Vehicle with Multiple Traction Motors by Particles Swarm Optimization," CACS International Automatic Control Conference, pp. 233–238 (2013).

(5) O. Nishihara and T. Kumazawa:"Minimization of energy consumption for an Electric Vehicle with driving force distribution," Dynamics and Deign Conference, pp. 330-1–330-6 (2010).

(6) X. Yuan, J. Wang and K. Colombage:"TORQUE DISTRIBUTION STRATEGY FOR A FRONT AND REAR WHEEL DRIVEN ELECTRIC VEHICLE," IEEE Trans. on Vehicular Technology, Vol. 61, No. 8, pp. 3365–3374 (2012).

(7) C. Yeo and T. Koseki: "Optimization of Running Profile of Train by Dynamic Programming," National Convention of IEEJ, Vol. 3, pp. 85-86 (2002).

(8) S. Egami and H. Fujimoto:"Range Extension Control System for Electric Vehicle Based on Front and Rear Driving Force Distribution Considering Load Transfer," in Proc. 37th Annual Conference of the IEEE Industrial Electronics Society, Melbourne, pp.3721–3726 (2011).

(9) S. Harada and H.Fujimoto:"Range Extension Control System for Electric Vehicles during Acceleration and Deceleration Based on Front and Rear Driving-Braking Force Distribution Considering Slip ratio and Motor Loss," in Proc. 39th Annual Conference of the IEEE Industrial Electronics Society, Vienna, Austria, pp. 6624–6629 (2013).

(10) S. Harada and H. Fujimoto: "Range Extension Control System Based on Optimization of Acceleration-Deceleration Trajectory and Front and Rear Driving-Braking Force Distribution ," Multi-symposium on Control Systems, 6F1-4 (2014) (In Japanese).

(11) Ministry of Land, Infrastructure, Transport and Tourism, Investigative commission on auto pilot system, "The realization of auto pilot system" http://www.mlit.go.jp/road/ir/ir-council/autopilot/pdf/torimatome/honbun.pdf (In Japanese).

(12) H. B. Pacejka and E. Bakker: " The Magic Formula Tyre Model, " Vehicle System Dynamics: International Journal of Vehicle Mechanics and Mobility , Vol. 21, No. 1, pp. 1–18 (1992).